Processing and nuclear localization of CRMP2 during brain development induce neurite outgrowth inhibition.

Véronique Rogemond, Carole Auger, Pascale Giraudon, Michel Becchi, Nathalie Auvergnon, Marie-Françoise Belin, Jérôme Honnorat, Mahnaz Moradi-Améli

PROCESSING AND NUCLEAR LOCALIZATION OF CRMP2 DURING BRAIN DEVELOPMENT INDUCE NEURITE OUTGROWTH INHIBITION

Véronique Rogemond‡§, Carole Auger‡, Pascale Giraudon‡, Michel Becchi¶, Nathalie Auvergnon‡, Marie-Françoise Belin‡, Jérôme Honnorat‡§ and Mahnaz Moradi-Améli‡

From: ‡Inserm, U 842, Lyon, France; Université de Lyon, Lyon 1, UMR-S842, Lyon, F-69372 France; §Hospices Civils de Lyon, Neurologie B, Lyon, France; ¶ Institut de Biologie et Chimie des Protéines, CNRS- UMR 5086, Lyon, F-69367, France

Running Title: Processed CRMP2 localization and function during development

Address correspondence to: M. Moradi-Améli, Tel: (33) 478 78 57 06; Fax: (33) 478 77 86 16; E-mail: mahnaz.ameli-moradi@univ-lyon1.fr; and J. Honnorat, Tel: (33) 472 35 78 08; Fax: (33) 472 35 73 29; E-mail: jerome.honnorat@chu-lyon.fr; at Inserm U842, Neuro-Oncologie et Neuro-Inflammation, Université de Lyon, Université Lyon 1, Faculté de médecine Laënnec, Rue Guillaume Paradin, 69372 Lyon cedex 08, France;

Collapsin response mediator proteins (CRMP) are believed to play a crucial role in neuronal differentiation and axonal outgrowth. Among them, CRMP2 mediates axonal guidance by collapsing growth cones during development. This activity is correlated with the reorganization of cytoskeletal proteins. CRMP2 is implicated in the regulation of several intracellular signaling pathways. Two subtypes A and B, and multiple cytosolic isoforms of CRMP2B with apparent masses between 62-66 kDa have previously been reported. Here, we show a new short isoform of 58 kDa, expressed during brain development, derived from C-terminal processing of CRMP2B subtype. While full-length CRMP2 is restricted to the cytoplasm, using transfection experiments, we demonstrate that a part of the short isoform is found in the nucleus. Interestingly, at the tissue level, this short CRMP2 is also found in a nuclear fraction of brain extract. By mutational analysis we demonstrate, for the first time, that nuclear translocation occurs *via* nuclear localization signal (NLS) within residues R471-K472 in CRMP2 sequence. The NLS may be unmasked after C-terminal processing, thereby, this motif may be surface-exposed. This short CRMP2 induces neurite outgrowth inhibition in neuroblastoma cells, and suppressed axonal growth in cultured cortical neurons, while full-length CRMP2 promotes neurite elongation. The NLS-mutated short isoform, restricted to the cytoplasm, abrogates both neurite outgrowth and axon growth inhibition, indicating that short nuclear CRMP2 acts as a dominant signal. Therefore, post-transcriptional processing of CRMP2 together with its nuclear localization may be an important key in the regulation of neurite outgrowth in brain development.

INTRODUCTION

Collapsin response mediator proteins (CRMP) constitute a family of five cytosolic proteins, abundantly expressed in the developing nervous system, but down regulated in the adult brain. They play important roles in neurite outgrowth and axonal guidance (1, 2). Among them, CRMP2 was originally identified as a signaling molecule, required for growth cone collapse of dorsal root ganglion neurons, in response to a repulsive guidance cue, semaphorin-3A (Sema-3A) (2). CRMP2 was also reported to have a positive effect on axonal extension and to play a crucial role in axon-dendrite specification and axon regeneration, since the overexpression of

CRMP2 induces the formation of multiple axons, and the expression of the dominant-negative form of CRMP2 or the knockdown of CRMP2 suppresses axon formation (3-7). Morphological changes and the motility of neuronal growth cones are closely related to the reorganization of actin, tubulin, and other cytoskeletal proteins (8, 9). Accordingly, CRMP2 co-localizes with F-actin in the growth cones of different types of neurons (1, 2, 10). Moreover, CRMP2 is thought to regulate axonal growth through its interaction with tubulin dimers to promote microtubule assembly. The CRMP2-tubulin interaction seems to be mediated by a microtubule-binding domain, spanning amino acids 323-381 within CRMP2 (4). Besides, CRMP2 was shown to bind to the kinesin-1 light chain (KLC), thereby regulating the transport of soluble tubulin to the distal parts of growing axons (11). By interacting with the Sra-1/Wave1 complex (Rac1-associated protein 1/WASP family verpolin-homologous protein 1), CRMP2 operates by transporting it to the growth cone of axons *via* KLC (12). CRMP2 also participates in the polarized Numb-mediated endocytosis of the neuronal adhesion molecule L1 at the growth cones (6). Besides the above-mentioned proteins, other CRMP2-interacting molecules such as chimaerin and phospholipase D have also been identified (13, 14).

In parallel, our group has shown that CRMP2 may act as a regulator of other functions such as migration and proliferation, since CRMP2 is highly expressed in the developing cerebellum, either in the proliferative external granular layer or in growing fibers in the molecular layer (15). Collectively these data indicate that by interacting with different molecular partners, CRMP2 may play a pivotal role in regulating several signaling pathways leading to nervous system development.

A number of studies have raised the possibility that post-translational modifications of CRMP2 modulate its activity in axonal growth or growth cone dynamics, by preventing its association with other molecules. There is growing evidence that CRMP2-tubulin interaction is regulated by CRMP2 phosphorylation, which inhibits the ability of CRMP2 to promote microtubule assembly, and induces growth cone collapse, suggesting that the phosphorylation states of the CRMP2 modulate its activity (7, 16-18). On the other hand, hyperphosphorylation of CRMP2 is implicated in some pathology such as Alzheimer's disease (16, 19, 20). However, beside phosphorylation, other post-translational modifications may exist, which regulate the function of CRMP2.

CRMP2 has the characteristic of being present under different isoforms (21), however, little is known about the function of each isoform. Two subtypes (A and B) have been reported for different CRMPs (1-4), derived from alternative splicing of their N-terminal region (10). We reported that CRMP2A, present as a 75 kDa protein, was specifically localized in neuronal soma and/or axons but was absent from dendrites, while CRMP2B was localized in both axons and dendrites (21). The balance between the expressions of the two subtypes is involved in the control of axon branching and elongation. CRMP2B is present in different isoforms with apparent masses varying between 62 and 66 kDa (10, 19, 21). Despite extensive studies on CRMP2 during the last few years, no attempt has been made to elucidate the spatio-temporal expression and the function of each of these multiple isoforms of CRMP2. Recently, another isoform (58 kDa) resulting from post-translational processing of CRMP2 and of CRMP4 have been reported after brain injury such as ischemia (21-24). We showed an NMDA-induced post-translational processing of CRMPs, including CRMP2, in cortical neurons also leading to the appearance of short isoform (25).

Because CRMP2 exerts various functions depending on its post-translational modification state, an insight into the spatio-temporal expression and the function of the 58 kDa short isoform offers an important key to elucidating the role of this isoform in neuronal development. In the present study, we show, the developmental-dependent expression of a short isoform (58 kDa) of CRMP2 exclusively present in the embryonic and post-natal stages, but absent in adult brain. We show that, this short isoform derives from post-translational C-terminal processing of CRMP2B subtype, thus, unmasking a nuclear localization signal (NLS) within CRMP2. This short isoform is found in the nucleus, at both cellular and tissular levels. We define, for the first time, a functional NLS sequence within the CRMP2 isoform. The nuclear short CRMP2 induces neurite outgrowth inhibition, thereby, suggesting that CRMP2 plays an important role in the regulation of neurite outgrowth in brain development.

EXPERIMENTAL PROCEDURES

Crude brain extract— Adult male, post-natal days 1 (P1) 5 (P5) and 15 (P15), rats or mice (OFA, Charles River laboratories, L'Arbresle, France) were anesthetized with pentobarbital. Embryos at embryonic days 14 (E14), 16 (E16) and 19 (E19) were removed from anesthetized pregnant females. After decapitation, the brains were removed and chilled on ice. All subsequent steps were performed at 4 °C. Cerebral tissues were sonicated in 10 mM Tris-HCl, pH 7.4, 0.02% sodium azide, 1 mM EDTA, 0.2% Triton X-100 supplemented with protease inhibitor cocktail (Complete, Roche, France) and centrifuged for 10 minutes at 2000 × g at 4 °C. The proteins in the supernatant were quantified (Coomassie Plus Protein Assay Reagent, Pierce), diluted to a concentration of 6 mg/ml in the homogenization buffer and stored at –80 °C until used.

Subcellular fractionation— Cerebella of post-natal rats (P1) were explanted and cleaned free of meninges, and subjected to subcellular fractionation using the proteoExtract subcellular Proteome extraction Kit from Calbiochem (vWR, Fontenay, France) following exactly the manufacturer's instructions. Briefly, 50 mg of tissue were resuspended in 1 ml of extraction Buffer I and incubated for 10 min at 4 °C under gentle agitation. After centrifugation for 10 min at 1000 × *g*, the supernatant containing cytosolic fraction was kept apart. Then, the pellet was resuspended in 1 ml of extraction Buffer II, incubated for 30 min at 4 °C, and the suspension was centrifuged for 30 min at 6000 × *g*. The supernatant, containing membrane protein fraction, was kept apart, and the pellet was incubated with 500 µl of Buffer III containing 375 units of Benzonase (Calbiochem) for 10 min at 4 °C under gentle agitation. Another centrifugation at 10.000 × *g* allowed the separation of nuclear protein remaining in the supernatant. The pellet, dissolved in 500 µl of Buffer IV, allowed the recovery of the cytoskeletal fraction. All buffers contained 5 µl of inhibitor cocktail.

Antibodies used and western blot analysis— The site-specific antibodies to CRMP2 were obtained as previously described (21, 26). The peptide sequences used to generate specific antisera were ^{557}IVAPPGGRANITSLG^{572} targeting the CRMP2 C-terminal region (C-ter), and ^{454}LEDGTLHVTEGS^{465} (pep 4). Peptides were conjugated to keyhole limpet hemocyanin and used to immunize rabbits. The anti-peptide antibodies (IgG) were purified by affinity chromatography on the corresponding immobilized peptide. Extracts from brain or transfected cells (30 µg) were diluted in Laemmli sample buffer, resolved by SDS-PAGE (8% or 10% polyacrylamide gels), transferred onto a polyvinylidende difluoride (PVDF) membrane, and incubated with different antibodies was as described (25). The target protein was detected using

diaminobenzidine as peroxidase substrate or an enhanced chemiluminescence (ECL) detection system (Covalab, Lyon, France) and x-ray film. Densitometric quantification of the immunoblot bands was performed using Image Quant (Molecular Dynamics).

Protein preparation, in-gel enzymatic proteolysis, and mass spectrometry— A 300 µl aliquot of the cytosolic fraction from mouse brain cortex was dialyzed against 25 mM Tris-HCl, pH 7.4, 1 mM EDTA, 1 mM DTT, 5 mM $MgCl_2$, and 10 mM PPi and applied to 1 ml Q-Sepharose columns (Hi-trap Q, GE Healthcare). After elution with 0.5 M NaCl, in the same buffer, CRMP2-enriched fractions were pooled and concentrated on an Ultrafree Biomax membrane (Millipore), dialyzed, then subjected to SDS-PAGE (8% polyacrylamide). Protein bands were stained with Coomassie blue, according to standard protocols, the bands of interest excised from the gel, and in-gel digestion with trypsin was carried out as described by Shevchenko *et al.* (27) with minor modifications. Tryptic peptides were analyzed by matrix-assisted laser desorption/ionization time-of-flight mass spectrometry (MALDI-TOF MS), using a Voyager DE-PRO workstation (Applied Biosystem, Courtaboeuf, France). Spectra were recorded in the mass range 700-5000 Da. A 200 µl solution of 0.5% α-cyano 4-hydroxycinnamic acid (LaserBioLab, Sophia-Antipolis, France) in 50% acetonitrile, 50% H_20, and 0.1% TFA was used as matrix. The instrument was calibrated using trypsin autolysis fragments at m/z 842.5100 and 2211.1046 Da. Peptide mass fingerprinting was compared to the theoretical masses from the SwissProt sequence database using Protein Prospector MS-Fit software. Typical search parameters were as follows: ±40 ppm of mass tolerance, carbamidomethylation of cysteine residues, methionine considered in oxidized form, one missed enzymatic cleavage for trypsin, a minimum of five peptide mass hits was required for a match and a protein mass range from 5 to 100 kDa was permitted. Probability-based molecular weight search (MOWSE) scores greater than 1000 were considered as significant.

Database and Structure analysis— Sequences were aligned using the CLUSTAL program (28). The prediction programmes PROSITE (http://us.expasy.org/prosite) and PSORT II (http://cubic.bioc.columbia.edu/predictNLS) were used to identify putative NLS. The online prediction program at: http://cubic.bioc.columbia.edu/service/NORSp was used to identify the Intrinsically Unstructured Protein (IUP)-related structure of the C-terminal part of CRMP2. The structure of CRMP2 was modeled, based on the coordinates available for CRMP2 chain D (protein Data Bank entry 2GSE), using Viewerlite/4.2 (Accelrys).

Expression constructs, cell culture and transfection— Full-length CRMP2 or the C-terminally truncated ΔC503 were amplified by PCR and inserted directionally into the pCMV2-FLAG vector (Sigma, L'Isle d'Abeau, France), which generated a protein with a FLAG-tag at its N-terminus. A two steps PCR procedure was used for the CRMP2 ΔC503 mutants preparation. First, C-terminal fragments were generated using ΔC503 reverse primers introducing an *Eco R1* site at the 3' end, and forward primers with substituted codons as follows: mutant 1, R471 (CGG) and K472 (AAG) both substituted with A (GCG); mutant 2, K480 (AAA) and R481 (CGC) substituted with A (GCA) and A (GCC) respectively; mutant 3, K483 (AAG), R485 (AGG) and R487 (AGG) substituted each with A (GCG). Next, the three mutated fragments were used as reverse primers in the PCR reaction with a wild type forward primer introducing a *Hind III* site at the 5' end. For the full-length mutant R471-K472, two overlapping PCR products bearing the mutated codons (nucleotides 1-1506, and 1387-1716) were first obtained by separated reaction using wild-type CRMP2 as template. Fragment 1-

1506 corresponded to ΔC503 mutant 1. Fragment 1387-1716 was generated using a mutagenic forward primer introducing the above-mentioned substituted codons and a wild-type reverse primer. Both fragments were mixed, then allowed to hybridize (5 min at 50 °C) and elongate (10 min at 70 °C) for the generation of the mutated template. Finally, this template was used in a last PCR step to generate full-length mutated CRMP2, using the above described forward and reverse CRMP2 primers introducing *Hind III* and *Eco RI* sites. The correct DNA sequences of all constructs were verified. The final PCR product was cloned into the *Hind III* and *Eco RI* sites of the pCMV2-FLAG vector. PC12 cells were transfected by 2 μg of purified plasmid using the Amaxa nucleofector reagent and electroporation, following precisely the manufacturer's protocol. N1E-115 cells were seeded in 10% fetal bovine serum containing medium and cultured overnight. The cells were transiently transfected, in the absence of serum, using LipofectAMINE LTX (In Vitrogen) essentially as described (4, 5). Twenty-four hours post-transfection, cells were cultured in 5% serum containing medium for 24 h and were treated for immunohistochemistry analysis. Cortical neurons from E15 mouse embryos were prepared as described (29). Dissociated cells were seeded on plastic dishes coated overnight with 1.5 μg/ml poly-D-ornithine in chemically defined Dulbecco's modified Eagle's/F12 medium free of serum with 2 mM glutamine, 9 mM $NaHCO_3$, 10 mM HEPES, and 33 mM glucose. The medium was supplemented with hormones and proteins (100 μg/ml transferin, 25 μg/ml insulin, 20 nM progesterone, 60 μM putrescin, 0.1% ovalbumin, and 30 nM Na selenite). After 3 days of *in vitro* culture, neurons were transfected using LipofectAMINE LTX (In Vitrogen) in medium without hormones and proteins. Twenty-four hours post-transfection, neurons were cultured in the presence of hormones and proteins for a further 48h.

Immunofluorescence study and microscopic observation— The PC12 cells were observed 48 h after transfection using a laser scanning confocal system (Leica TCF SP2, Austria) imaging platform. The cells were fixed in 4% paraformaldehyde for 20 min, washed in PBS, blocked with PBS containing 2% gelatin and 0.1% Triton X-100, before incubation with different antibodies. The cells were double-stained with polyclonal anti-FLAG (Sigma F 7425) and anti-rabbit Alexa Fluo 488 (In Vitrogen) antibodies and with monoclonal anti-α tubulin (Sigma) and anti-mouse Cy3 (Jackson) antibodies. For some experiments, an anti-rabbit Alexa Fluo 546 (In Vitrogen) was used. Nuclei were visualized by DAPI staining, and Alexa Fluo 546-Phalloidin (In Vitrogen) was used for F-actin staining. For morphometric analysis, both N1E-115 cells and mouse embryo cortical neurons transfected with FLAG-CRMP2 (full-length, Δ503, and mutant 1) were viewed using the Axioplan II fluorescence microscope (Carl Zeiss). N1E-115 cells were fixed and stained with polyclonal anti-FLAG and anti-rabbit Alexa Fluo 488 antibodies. The percentage of cells bearing neurites (length >20 μM from the cell body) among the transfected cells was measured. At least 300 cells for each expressed protein from three different experiments were examined. Cortical neurons were fixed and visualized by immunostaining with anti-FLAG antibody. Non-transfected cortical neurons, used as control cells, were stained by anti-pep4 and anti-rabbit Alexa Fluo 488 antibodies. The length of the longest neurite was measured as that of an axon, and compared to axon length of control neurons. At least 40 cells for each expressed protein were examined in one experiment. The axon length from three different experiments was examined.

RESULTS

Identification of different isoforms of CRMP2 during brain development— To study different isoforms of CRMP2, a site-specific antibody recognizing residues 454-465 of CRMP2 was used (anti-pep 4, Fig. 1A). The specificity of this antibody towards CRMP2, but not CRMP1, 3, 4, and 5 had previously been confirmed (26). Besides the well-known and abundant 64 kDa CRMP2, other isoforms of CRMP2 migrating as 62 and 66 kDa could be detected in embryonic brain extract as faint bands (Fig. 1C, anti-pep4), their intensity increasing at the post-natal stages. The presence of such isoforms was reported in previous studies (19). However, in embryonic brain cortex, an additional isoform presenting an apparent mass of 58 kDa was recognized by the anti-pep4 antibody (Fig. 1C). To determine whether the presence of this short isoform of CRMP2 is a development-dependent process, it was searched for in brain extracts at embryonic and early post-natal stages. As an internal loading control, the extent of actin was checked in all lanes using anti-actin antibody (data not shown). Anti-pep4 antibody clearly recognized a band migrating at 58 kDa in the cortex extract from embryo (stages E14, E16, and E19), as well as in the extract of early post-natal P1-P15 brain (Fig. 1C, anti-pep4). The intensity of this band decreased gradually during development since only a faint band was recognized by the anti-pep4 antibody at stage P15 (Fig. 1C and D), while other isoforms (62-66 kDa) of CRMP2B were clearly detected (Fig. 1C). As shown in Fig. 1D, the ratio of 58 kDa band to 64 kDa decreased at late stages of brain development. This 58 kDa band was also detected by anti-pep4 antibody in an extract from primary cortical neuron cultured at stage E15 (Fig. 1B). In addition, a high molecular mass band (75 kDa) belonging to CRMP2A could be visualized from the P1 stage onward (Fig. 1C). On the other hand, in adult brain, the 58 kDa band was almost absent, since a very faint band, presenting very low intensity, could be detected by the anti-pep4 antibody. However, significant intensity was detected for the 64 kDa isoform (Fig.1C and D).

The appearance of the 58 kDa band suggests that it may be the result of cleavage of the longer 62-66 kDa forms. Therefore, we used another site-specific anti-peptide antibody (21) designed to recognize the most C-terminal residues (558-572) of CRMP2 (Fig. 1A). While the anti-C-ter antibody detected all the higher molecular mass isoforms of CRMP2 (Fig. 1C, anti-C-ter), strikingly, it failed to recognize this 58 kDa isoform at all the above-mentioned developmental stages (E14-P5). These data indicate that this short isoform is a processed form of CRMP2 lacking at least the most C-terminal residues.

Characterization of the short isoform of CRMP2— To further characterize the short form of CRMP2, four different tissue isoforms presenting masses of 58, 62, 64, and 66 kDa were compared by proteomic analysis. After separation by SDS-PAGE, protein bands corresponding to 58, 62, 64, and 66 kDa were excised and subjected to in-gel trypsin digestion. The resulting tryptic peptides from each gel piece were analyzed by MALDI-TOF mass spectrometry (Fig. 1E). Monoisotopic peptide masses were matched with the theoretical peptide masses of proteins from mammalian species as found in the Swiss Prot database, allowing a mass tolerance of 40 ppm (30 ppm for 58 kDa). Unmatched peptides were not considered. High probability-based MOWSE scores of 4.1×10^{6}, 2.6×10^{5}, 3.4×10^{8}, and 3.6×10^{4} were obtained for the protein bands of 58, 62, 64, and 66 kDa, respectively, ensuring the identity of these proteins as CRMP2. MALDI-TOF analysis showed the presence of many identical tryptic cutting sites among the four isoforms (Fig. 1, E and F). However, through comparative analysis of the peptide sequences, we found that peptides encompassing residues 558-565, present in three isoforms (62, 64, 66 kDa) were not

contained in the short 58 kDa CRMP2 tryptic sequences. Moreover, residues 533-552, present in two isoforms (64 and 66 kDa), were also absent from the short 58 kDa sequence.

These data indicate the cleavage of both amino acid sequences 533-552 and 558-565 in the 58 kDa form (Fig. 1, E and F). Although present in both 64 and 66 kDa isoforms, the tryptic peptide 526-532 was detected only in 62 kDa, so its presence or absence in the 58 kDa form could not be elucidated. The most C-terminal sequence that 58 kDa and other CRMP2 isoforms (64 and 66 kDa) have in common is 472-481. These results confirm the C-terminal processing of the short CRMP2 isoform, and suggest that cleavage occurs N-terminal to the residue 533 within residues 481 to 532. The absence of any tryptic sequence corresponding to CRMP2A at the N-terminus, bearing many tryptic cutting sites, suggests that the short isoform is a cleavage product of the CRMP2B subtype, hereafter referred to as CRMP2.

Distributional analysis of the over-expressed short isoform of CRMP2— To further explore the localization of CRMP2, we performed confocal analysis on PC12 cells transfected with FLAG-tagged expression vectors containing either wild-type full-length CRMP2 (1-572) or truncated CRMP2 ΔC503 (1-502). The truncated ΔC503 was designed (Fig. 2A) to mimic the short isoform, containing the last peptide sequence (472-481) previously determined on the short 58 kDa isoform by mass spectrometry. The efficiency of CRMP2 transfection was about 15% and 25% for the full-length and truncated forms, respectively. In a set of experiments, the cells were transfected with an empty plasmid vector as a control. To ascertain the correct protein expression after transfection, PC12 cells extract was subjected to Western blot analysis using anti-FLAG antibody. As expected, the truncated CRMP2 showed faster migration than the full-length CRMP2, the migration of both bands corresponding to their respective molecular masses, and the absence of FLAG-tagged CRMP2 can be noticed after transfection with the empty plasmid vector (Fig. 2B). After 48h, the transfected cells were immunostained with anti-FLAG antibody (green stained) and phalloidin to label CRMP2 and the F-actin, respectively (Fig. 2C). CRMP2 immunoreactivity was localized at the cytoplasmic level in 100% of FLAG-tagged CRMP2 expressing cells (n= 49), where a clear co-localization of full-length CRMP2 with actin was observed (Fig. 2C, merge), as previously reported for chick DRG. No immunostaining with anti-FLAG was observed for cells transfected with empty vector. The truncated ΔC503 was diffusely distributed in the cytoplasm, but, as observed in high magnification of the merged image (Fig. 2C) no co-localization with actin was observed (n=103), suggesting that the short CRMP2 isoform might not contain either an actin binding domain or be associated with actin-binding partners. Since tubulin is known to co-localize with CRMP2 (4), a double immunostaining was performed with α-tubulin (Fig. 2D). Full-length CRMP2 (n=50), as well as ΔC503 (n=50), co-localized with tubulin at the cytoplasmic level (Fig. 2D, merge). Co-localization of truncated ΔC503 and tubulin was expected since the truncated CRMP2 bears the tubulin-binding domain mapped within residues 323-381 (4).

These results, in agreement with previously reported data on the localization of wild-type CRMP2 in neurons, validated this model for the further study of the nuclear localization of CRMP2. We examined the immunoreactivity of both forms of CRMP2 using an anti-FLAG antibody (red stained) and counterstaining with DAPI to label the nucleus. The merged image in Figure 2E shows unambiguously that the full-length isoform of CRMP2 presents exclusively a cytosolic distribution in 100% of tagged CRMP2 expressing cells (n=46). In contrast, ΔC503 presents a nuclear distribution (n=59) as well as a cytoplasmic one, as

observed by the red staining of the cytosol and the nucleus in Figure 2E. It is worthwhile noting that, upon close examination, nuclear staining of ΔC503 can also be observed in Figure 2, C and D after immunolabelling with anti-FLAG antibody (green stained). An overall of 85% of nuclear staining was observed within at least 300 CRMP2 ΔC503 transfected cells examined in Figure 2C, D, and E.

Identification of a functional NLS within CRMP2— To understand the mechanism of the nuclear translocation of this short isoform, we searched for the presence of any nuclear targeting signals in the CRMP2 sequence. Database analysis of the 572 amino-acid sequence of CRMP2 using protein domain prediction programs (PROSITE, and PSORT II) indicated the presence of a bipartite nuclear localization signal (NLS) within residues 471-487 (Fig. 3A). The peptide sequence conformed to the sequence required for bipartite NLS, as shown by sequence alignment with the bipartite NLS motif in other nuclear proteins (Fig. 3B). To assess the functional significance of the NLS motif, we engineered mutations within this motif on the short CRMP2B ΔC503, transiently transfected these mutants into PC12 cells, and studied their effects on the nuclear localization of CRMP2 ΔC503 using confocal fluorescence microscopy (Fig. 3C). The FLAG-tagged CRMP2 ΔC503 mutants K480A + R481A (mutant 2), and K483A + R485A + R487A (mutant 3) retained nuclear localization in addition to their cytoplasmic distribution, since, a red staining of the nucleus similar to that observed with CRMP2 ΔC503 was detected (compare Figs. 2E and 3C). Therefore, the putative bipartite NLS motif at residues 480-487 is non-functional. In contrast, the ΔC503 R471A + K472A mutant 1 which disrupts the two key positively charged residues on the N-terminal side of the NLS motif prevented nuclear translocation since it showed cytoplasmic distribution, demonstrating that this domain of CRMP2 contained a functional NLS (Fig. 3C). Therefore, these results demonstrate that CRMP2 has a functional monopartite NLS that conforms to monopartite motifs characterized by positively charged residues, which are preceded by a helix-breaking residue (P470). This motif consists of the key RK residues 471-472.

Based on the CRMP2 coordinates available for fragment 13-490 (30), we illustrated the position of amino acids 471-487 (Fig. 4, colored green) within determined structure of CRMP2. Surface exposure for the α helix encompassing residues 474-489 has been reported (30). Strikingly, functional NLS residues 471-472, located N-terminal to this α helix, remain in a flexible unconstrained conformation, and are also well exposed at the surface of CRMP2 (insert Fig. 4). Nonetheless, the structure of CRMP2 C-terminal to residue 490 remained unsolved in the x-ray structure, so we searched for the structure of the C-terminal part of full-length CRMP2 using the NORS prediction program (see *Experimental Procedures*). We found that this C-terminal region (residues 489-572) belonged to "Intrinsically Unstructured Proteins" (IUP)" permitting a malleable structural state. This is the first report mentioning the presence of such an unstructured region in CRMP2. Such a flexible region may mask the NLS motif in the full-length CRMP2. The short CRMP2 isoform is devoid of at least half of this unstructured region. These data suggest that the nuclear localization of the short isoform of CRMP2 may occur by the surface-exposure of an NLS motif after removal of the flexible C-terminal region of full-length CRMP2.

Tissue localization of short CRMP2 isoform— To shed light onto the localization of the short form of CRMP2 at the brain tissue level, different subcellular fractions of an extract of rat cerebellum at P1 stage, were prepared and subjected to western blotting (Fig. 5, upper level) using anti-pep4 antibody and specific

antibodies to different fractions. Although not present in equal amounts, different isoforms of 62, 64, and 66 kDa were detected in the cytosolic and membrane fractions by the anti-pep4 antibody, but these isoforms were absent from nuclear fractions and the cytoskeleton. The subcellular identification of each fraction was ascertained by the specificity of antibody recognition and the absence of antibody cross-reactivity toward non-relevant fractions (Fig. 5 bottom levels). The short 58 kDa CRMP2 isoform was essentially detected in the nuclear fraction, although a faint band was detected in the cytosolic fraction (Fig. 5). It should be noted that, the nuclear fraction was exclusively recognized by specific anti-histone H1 antibody, indicating that this fraction is devoid of any contamination with other fractions such as cytosol, membrane or cytoskeleton. These results reinforce the above data on the nuclear localization of CRMP2, and demonstrate that, the processed short form of CRMP2 extracted from brain, is located in the nucleus. The nuclear localization of CRMP2 is a developmental-dependent process, since anti-pep4 immunolabeling of rat brain sections showed, unambiguously, high CRMP2 expression at the nucleus in cerebellum and cortex at P1 stage, and the absence of nuclear labeling in adult brain (supplemental Fig. S1, A and B). In addition, at P1 stage, the lack of nuclear labeling by anti-C-ter antibody confirmed the nature of the nuclear CRMP2 as short CRMP2 isoform (supplemental Fig. S2, A and B). In the adult cortex, CRMP2 was exclusively expressed in the cytosol, while not detected in the cerebellum (supplemental Fig. S1, A and B). This new localization is in addition to that previously reported for CRMP2 in the plasma membrane (31).

Function of the short isoform of CRMP2—To delineate the biological function of the short CRMP2 isoform, we investigated the effect of short CRMP2 expression on neurite outgrowth representing one of the multiple functions reported for CRMP2. We transfected the N1E-115 neuroblastoma cells with FLAG-tagged full-length or short ΔC503 CRMP2 constructs and examined the length of neurites formed after transfection (Fig. 6A). In a set of experiments, the cells were transfected with empty constructs as negative control in which no neurite formation can be seen (Fig. 6B). The efficiency of the transfection was about 25%. Full-length CRMP2 induces neurite outgrowth concomitant with the appearance of polygonal cells (Fig. 6A). The percentage of transfected cells presenting longer neurites above 20 μm is concordant with that previously reported (5). On the other hand, short CRMP2 ΔC503 constructs displayed significantly less neurite elongation (Fig. 6, A and C) and short microspike-like processes were seen on the cells, which present an overall round shape. To elucidate whether this attenuation of the neurite elongation of ΔC503 CRMP2 was related to the nuclear localization of the protein, N1E-115 cells were transfected with the ΔC503 R471A+K472A mutant bearing the mutation that disabled the nuclear translocation of the short protein. This mutation restored, clearly, the neurite elongation activity of CRMP2, since the N1E-115 cells presented neurite outgrowths comparable to full-length CRMP2 (Fig. 6, A and C). No additional induction of neurite elongation could be attributed to this mutation, since similar extent of neurite outgrowth was observed after transfection of N1E-115 cells with a mutated full-length CRMP2 bearing R471A+K472A mutation (Fig. 6, A and C). We further investigated the function of short CRMP2 isoform on the regulation of axonal growth in cortical neurons. Cortical neurons from E15 embryo were transfected with different FLAG-tagged constructs. As shown in Fig. 7 (A and B) the length of primary axons in neurons expressing full-length CRMP2 was longer (1.6 fold) than that of non-transfected neuronal cells, which expressed endogenous CRMP2. On the contrary, the mean length of processes, assumed as axons, from cells

expressing Δ5C03 was the shortest among the cells examined (Fig. 7A), and there was significant difference between the control cells expressing endogenous CRMP2 and the ΔC503 construct (Fig. 7B). The expression of ΔC503 R471A+K472A mutant in neurons increased the length of primary axon when compared to the control. Besides, the expression of ΔC503 construct in neurons significantly reduced the number of cells bearing longer neurites, since only 6% of ΔC503 CRMP2 transfected neurons presented long processes, while this percentage reached 50% for the neurons transfected with full-length and ΔC503 R471+K472 mutant constructs (data not shown). Taken together, these data indicate that short CRMP2 inhibited neurite formation and axonal growth, and that this activity was dependent on the nuclear localization of the short CRMP2.

DISCUSSION

Among CRMPs, CRMP2 is present in multiple forms derived from either alternative splicing or post-translational modification of the molecule. One of these forms consists of a short isoform of 58 kDa, previously reported for CRMP2, and identified as a C-terminally processed form, upon activation of calpain in response to NMDA activation or following brain injury. The production of calpain-induced form was co-related with a decrease of higher molecular mass isoform (23-25, 32, 33). Similar short isoform was also reported for CRMP4 (22). It is worth noting that in all the above reports, short isoforms were observed under conditions reminiscent of brain injury. Only one report identified a short CRMP2 isoform, under normal condition, in the peripheral side of spinal nerves (34).

Spatio-temporal expression of short isoform of CRMP2 during brain development — We first studied the presence and the localization of short isoform at the brain tissue level. We found that the 58 kDa short isoform of CRMP2 appeared during normal brain development, and, strikingly, was targeted to the nucleus. This is the first report on the nuclear targeting of a short isoform of CRMP2 in the central nervous system, specifically, in a context of normal brain development. The tissular 58 kDa isoform was the result of C-terminal processing of CRMP2 occurring within residues 481-532. Similar patterns of cleavage have been reported for CRMP2 in rat brain with different cleavage sites localized within residues 499-500 in traumatic brain injury (33) or residues 529-532 in focal cerebral ischemia (23). Consistently, in the peripheral side of spinal nerves, the truncated CRMP2 was devoid of at least a fragment of 7 amino acids in its C-terminal region (34). It is worth noting that in previous studies on C-terminal processing of CRMP2 and 4, the CRMP subtype was not identified (22-25, 32-34). In this study, the absence of any tryptic sequence corresponding to CRMP2A, together with the fact that the apparent mass of 58 kDa corresponded to a calculated mass based on the CRMP2B sequence, strongly suggested that the short isoform was a cleavage product of the CRMP2B subtype.

Subcellular localization of short CRMP2 isoform — We examine the localization of the full-length and short forms of CRMP2 by transient transfection of full-length or C-terminally truncated (ΔC503) CRMP2 in PC12 cells. The CRMP2 ΔC503 bearing half of the residues within the processing zone, may best mimic the tissular 58 kDa isoform. The co-localization of CRMP2 ΔC503 and tubulin emphasized their possible interactions, as observed for full-length CRMP2 (4), supporting its role in microtubule assembly. In contrast, CRMP2 ΔC503 showed localization different from that of actin, suggesting that the cytoplasmic short CRMP2 does not have a role in cytoskeletal changes. Therefore, the co-localization of full-length CRMP2 with actin may suggest that, the C-terminal region present in this molecule plays a role in actin binding, directly or indirectly *via* the formation of a

ternary complex. Similarly, it has been reported that the 100 C-terminal amino acids of CRMP4 contribute to the actin bundling of CRMP4 molecules (35). Strikingly, while full-length CRMP2 was restricted to the cytoplasm, CRMP2 ΔC503 was, unambiguously, localized in the nucleus when transfected into PC12 cells. However, as mentioned above, after transfection short CRMP2 remained partly cytoplasmic. Within few studies reporting the presence of CRMP2 in non-neuronal cells (36, 37), one report mentioned a leakage into the nuclear compartment observed after C-terminal truncation of CRMP2 in fibroblasts (37).

Nuclear signaling of CRMP2— The nuclear localization was observed not only at the cellular level, but also at the brain tissue level during development, underlying a natural biological function for the short CRMP2 molecule. To be imported into the nucleus, proteins need to be actively transported through the nuclear pore *via* a process dependent on the recognition by the importins of a nuclear localization signal (NLS) in the protein (38). We defined an NLS motif on CRMP2 within residues R471- K472, which acts as a signal for the active nuclear transport of CRMP2 ΔC503. Mutants harboring mutations at K480, R481 and at K483, R485, and R487, retained their nuclear localization, thereby further confirming that the above residues are not part of NLS, and that short CRMP2 bears a monopartite NLS. The NLSs do not conform to a specific consensus sequence, and are characterized by a cluster of positively charged residues preceded by a helix-breaking residue. Although the NLS, determined in this study, is shorter than the paradigmatic classical NLS (39), it is preceded by the helix-breaking residue P470. On the other hand, in accordance with our data, recent findings on the nuclear protein, parafibromin, showed a functional NLS formed by two basic residues (40). Furthermore, by molecular modeling of the recently determined CRMP2 structure (30), we showed that residues R471-K472 are exposed at the surface of the short isoform of CRMP2 and are under an extended conformation, which would be appropriate for binding to the super helix of the importin-α chain (41). CRMP2 have been reported to undergo oligomerization (30). Although, some residues of the C-terminal helix are engaged in CRMP2 oligomerization, it is worth mentioning that the NLS motif is not involved in the oligomerization interface. In the light of the tri-dimensional structure of CRMP2 (30), some findings concerning CRMP2 interaction with different partners were questioned, because the interacting region was buried within the CRMP2 molecule, but our findings here on the NLS signature are in accordance with those structural data.

The absence of translocation for the full-length CRMP2 also bearing the NLS signature may be due to the structure of the C-terminal part of the full-length CRMP2, which is not resolved in the crystal structure of CRMP2 (30). Using a predictional program, we found that the C-terminal part of CRMP2 (489-572) fell into the category of "Intrinsically Unstructured Proteins". The predictability of structural disorder from sequence, basically different from globular proteins, is well established in a vast majority of natively disordered regions (42). Such an unstructured state allows for the proteolytical susceptibility and flexibility of the molecule. Besides, such unfolded character being not able to adopt a compact state may be under an extended form (43). In full-length CRMP2 bearing the totality of this unstructured and extended region that constituted a bulky end, the NLS motif located close to this region, might be buried by it and therefore not accessible for nuclear targeting, while, in the processed short CRMP2 isoform, devoid of a part of this unstructured region, this motif may be exposed. However, its accessibility may not be total, explaining perhaps why a certain percentage of the short CRMP2 ΔC503 remains cytosolic.

Negative role of short CRMP2 in neurite elongation and axon growth— Under normal physiological conditions, CRMPs are downstream of semaphorin 3A receptors, encompassing neuropilin, plexin, and L1 subunits, and act as cytosolic mediators for axonal guidance by collapsing growth cones. The over-expression of full-length CRMP2 has been reported to promote neurite elongation and axon induction by modifying actin filaments and microtubules, and cytoplasmic flow (3-7). The function of short CRMP2 was not extensively studied, however, few studies, which have been reported on this function, presented contradictory results depending on the model and/or the conditions used. Under conditions reminiscent of brain injury, the overexpression of a cleaved form of CRMP2 on cortical neurons improved their resistance to NMDA cytoxicity (25), whereas the truncated CRMP2, in Hela cells, accelerated the appearance of apoptotic nuclei (37). However, we failed to detect any apoptotic activity after transfection with short CRMP2 ΔC503 in PC12 cells (unpublished observation). On the contrary, the transfection of the short isoform into N1E-115 cells promotes the inhibition of neurite elongation. Similarly, a decrease in primary axon length is observed in cortical neurons in culture expressing the short isoform. Thus, the nuclear short CRMP2 acts as a negative signal to stop neurite elongation. This signal is exclusively dependent on nuclear localization of the short CRMP2, since abrogation of nuclear translocation, by mutation of the NLS sequence, restores the neurite elongation activity of this molecule. This activity is strengthened by the fact that this mutant restores also axon outgrowth when expressed in cortical neurons. Therefore, the part of CRMP2 ΔC503**,** which remains cytoplasmic, may not exhibit any function since the neurite outgrowth inhibitory activity of nuclear protein appears dominant. Under normal physiological conditions, during brain development, a processing of CRMP2 takes place resulting in unmasking of NLS followed by nuclear translocation of the cleaved product. Nuclear proteins are involved in forming complexes that regulate genes that are involved in controlling cell differentiation and proliferation. Therefore, the short CRMP2 product translocated into nucleus may act as a regulator of transcriptional factors inducing gene expression leading to the inhibition of neurite outgrowth. Therefore, the balance between cytoplasmic full-length CRMP2 and post-transcriptionally processed forms of CRMP2 translocated to nuclear compartment may represent an important key in the regulation of neurite outgrowth during normal brain development**.**

ACKNOWLEDGMENTS

The authors thank Professor G. Deléage for the illustration of the CRMP2 structure, M. Touret for Western blot quantification, N. Chounlamountri and G. Cavillon for technical asistance.

REFERENCES

1. Minturn, J.E., Fryer, H.J., Geschwind, D.H. and Hockfield, S. (1995) *J. Neurosci.* **15,** 6757-6766
2. Goshima, Y., Nakamura, F., Strittmatter, P. and Strittmatter, S.M. (1995) *Nature* **376,** 509-514
3. Inagaki, N., Chuhara, K., Arimura, N., Menager, C., Kawano, Y., Matsuo, N., Nishimura, T., Amano, M. and Kaibuchi, K (2001). *Nat.Neurosci.* **4,** 781-782
4. Fukata, Y., Itoh, T.J., Kimura, T., Ménager, C., Nishimura, T., Shiromizu, T., Watanabe, H., Inagaki, N., Iwamatsu, A., Hotani, H.and Kaibuchi, K. (2002) *Nat. Cell Biol.* **4,** 583-591
5. Suzuki, Y., Nakagomi, S., Namikawa, K., Kiryu-Seo, S., Inagaki, N., Kaibuchi, K., Aizawa, H., Kibuchi, K. and Kiyama, H. (2003) *J. Neurochem.* **86,** 1042-1050
6. Nishimura, T., Fukata, Y., Kato, K., Yamaguchi, T., Matsuura, Y., Kamiguchi, H. and Kaibuchi, K (2003) *Nat Cell Biol.* **5,** 819-826
7. Yoshimura T., Kawano Y., Arimura N., Kawabata S., Kibuchi A. and Kaibuchi K. (2005) *Cell* **120,** 137-149
8. Buck, K.B. and Zheng, J.Q. (2002) *J. Neurosci.* **22,** 9358-9367
9. Zhou, F. -Q. and Cohan, C.S. (2004) *J. Neurobiol.* **58,** 84-91
10. Yuasa-Kawada, J., Suzuki, R., Kano, F., Ohkawara, T., Murata, M. and Noda, M. (2003) *Eur. J. neurosci.* **17,** 2329-2343
11. Kimura, T., Arimura, N., Fukata, Y., Watanabe, H., Iwamatsu, A. and Kaibuchi, K. (2005) *J. Neurochem.* **93,** 1371-1382
12. Kawano, Y., Yoshimura, T., Tsuboi, D., Kawabata, S., Kaneto-Kawano, T., Shirataki, H., Takenawa, T. and Kaibuchi, K. (2005) *Mol. Cell. Biol.* **25,**9920-9935
13. Lee, S., Kim, J.H., Lee, C.S., Kim, J.H., Kim, Y., Heo, K., Ihara, Y., Goshima Y., Suh, P.G. and Ryu S.H. (2002) *J. Biol. Chem.* **277,** 6542-6549
14. Brown, M., Jacobs, T., Eickholt, B., Ferrari, G., Teo, M., Monfries, C., Qi, R.Z., Leung T., Lim, L. and Hall, C. (2004) *J. Neurosci.* **24,** 8994-9004
15. Ricard, D., Rogemont, V., Charrier, E., Aguera, M., Bagnard, D., Belin, M.F., Thomasset, N. and Honnorat, J. (2001) *J. Neurosci.* **15,** 7203-7214
16. Cole, A.R., Knebel, A., Morrice, N.A., Robertson, L.A., Irving, A.J. Connolly, C.N. and Shuterland, C. (2004) *J. Biol. Chem.* **279,** 50176-50180
17. Arimura, N., Inagaki, N., Chihara, K., Ménager, C., Nakamura, N., Amano, M., Iwamatsu, A., Goshima, Y. and Kaibuchi, K. (2000) *J. Biol. Chem.* **275,** 23973-23980
18. Arimura, N., Ménager, C., Kawano, Y., Yoshimura, T., Kawabata, S., Hattori, A., Fukata, Y., Amano, M., Goshima, Y., Inagaki, M., Morone, N., Usukura, J. and Kaibuchi, K. (2005) *Mol. Cell. Biol.* **25,** 9973-9984
19. Gu, Y., Hamajima, N. and Ihara, Y. (2000) *Biochemistry* **39,** 4267-4275
20. Uchida Y., Ohshima, T., Sasaki, Y., Suzuki, H., Yanai, S., Yamashita, N., Nakamura, F., Takei, K., Ihara, Y., Mikoshiba, K., Kolattukudy, P., Honnorat, J. and Goshima, Y. (2005) *Genes Cell* **10,** 165-179
21. Bretin, S., Reibel, S., Charrier, E., Maus-Moati, M., Auvergnon, N., Thevenoux, A., Glowinski, J., Rogemond, V., Premont, J., Honnorat, J. and Gauchy, C. (2005) *J. Com. Neurol.* **486,** 1-17
22. Kowara, R., Chen, Q., Milliken, M. and Chakravarthy, B. (2005) *J. Neurochem.* **95,** 466-474
23. Chung, M.A., Lee, J.E., Lee, J.Y., Ko, M.J., Lee, S.T. and Kim, H.J. (2005) *Neuroreport* **16,** 1647-1653
24. Kobeissy, F.H., Otten, A.K., Zhang, Z., Liu, M.C., Denslow, N.D., Dave, J.R., Tortella, C., Hayes, R.L., and Wang, K.K.W. (2006) *Mol. Cell Proteomics* **5,** 1887-1898

25. Bretin, S., Rogemond, V., Marin, P. Maus, M., Torrens, Y., Honnorat, J., Glowinski, J., Prémont, J. and Gauchy C. (2006) *J. Neurochem.* **98,** 1252-1265
26. Quach, T.T., Duchemin, A.M., Rogemond, V., Aguera, M., Honnorat, J., Belin, M.F. and Kolattukudy, P.E. (2004) *Mol Cell Neurol*. **25,** 433-443
27. Shevenko, A., Wilm, M., Vorm, O. and Mann, M. (1996) *Anal. Chem.* **68,** 850-858
28. Higgins, D.G. and Sharp, D. (1988) *Gene* **73,** 237-244
29. Bouillot, C., Prochiantz, A., Rougon, G. and Allinquant, B. (1996) *J. Biol. Chem.* **271**, 7640-7644
30. Stenmark, P., Ogg, D., Flodin, S., Flores, A., Kotenyova, T., Nyman, T., Nordlund, P., and Kursula, P. (2007) *J. Neurochem.,* **101**, 906-917
31. Bulliard, C., Zurbriggen, R., Tornare, J., Faty, M., Dastoor, Z., and Dreyer, J.L. (1997) *Biochem. J.* **324,** 555-563
32. Jiang, S., Kappler, J., Zurakowski, B., Desbois, A., Aylsworth, A., and Hou, S.T. (2007) *Eur. J. Neurochem.* **26,** 801-809
33. Zhang, Z., Ottens, A.K., Sadasivan, S., Kobeissy, F.H., Fang, T., Hayes, R.L. and Wang, K.K.W. (2007) *J. Neurotrauma* **24,** 460-472
34. Katano, T., Mabuchi, T., Okuda-Ashitaka E., Inagaki, N., Kinumi, T. and Ito, S. (2006) *Proteomics* **6***,* 6085-6094
35. Rosslenbroich, V., Dai, L., Baader, S.L., Noegel, A.A., Gieselmann, V. and Kappler, J. (2005) *Exp. Cell Res*. **310,** 434-444
36. Vincent, P., Collette, Y., Marignier, R., Vuaillat, C., Rogemond, V., Malcus, C., Cavagna, S., Gessain, A., Machuca-Gavet, I., Belin, M.F., Quach, T. and Giraudon, P. (2005) *J. Immunol.* **175,** 7650-7660
37. Tahimic, C.G.T., Tomimatsu, N., Nishigaki, R., Fukuhara, A., Toda, T., Kaibuchi, K., Shiota, G., Oshimura, M. and Kurimasa, A. (2006) *Biochem. Biophys. Res. Commun.* **340,**1244-1250
38. Weis, K. (2002) *Curr.Opin. Cell Biol.* **14,** 328-335
39. Dingwall, C., and Laskey, R.A. (1991) *Trends Biochem. Sci*. **16,** 478-481
40. Bradley, K.J., Bow, M.R., Williams, S.E., Ahmad, B.N., Partridge, C.J., Patmanidi, A.L., Kennedy, A.M., Loh, N.Y. and Tahkker, R.V. (2007) *Oncogene* **26,** 1213-1221
41. Fontes, M.R.M., Teh, T. and Kobe, B. (2000) *J. Mol. Biol.* **297,** 1183-1194
42. Liu, J., and Rost B. (2003) *Nucleic acids Res.***31,** 3833-3835
43. Tompa P. (2005) *FEBS Lett.* **579,**3346-3354

FOOTNOTES

Abbreviations used: CRMP, collapsin response mediator protein; DTT, dithiothreithol; IUP, intrinsically unstructured protein; GSK-3β glycogen synthase kinase 3β; MALDI-TOF, matrix-assisted laser desorption/ionization time-of-flight; NLS, nuclear localization signal;

FIGURE LEGENDS

Fig. 1. Detection and characterization of a developmentally regulated short isoform of CRMP2. A, localization of antigenic peptides used to generate specific antisera, anti-pep4 and anti-C-ter, within the CRMP2 sequence. B, immunoblot analysis of CRMP2 expression in cortical primary neurons. Extract from 3 days culture of E15 cortical neurons embryos was immunoblotted with anti-pep4 antibody. C, down-regulation of a short 58 kDa CRMP2 protein during brain development. Extracts from embryonic brain cortex (stages E14, E16, E19), post-natal (stages P1, P5, P15), and adult (Adt) brain cortex were separated by SDS-PAGE and immunoblotted with either anti-pep4 or anti-C-ter antibody. Representative immunoblot from three independent experiments is shown. Strips were visualized by diaminobenzidine. Bars on the left indicate the position of apparent molecular marker bands. The arrows on the right indicate the apparent molecular mass of each separate isoform. The 75 kDa form belongs to the CRMP2A subtype. The thick arrow indicates the position of the short 58 kDa band. This band gradually disappears at late post-natal stages. Note that the anti-C-ter antibody failed to detect this band. D, quantitative densitometric analysis performed on the 58 kDa band detected in C by anti-pep4 antibody. Gel band intensity of 58 kDa at each developmental stage was quantified to derive its relative intensity. Data are expressed in arbitrary units. Error bars represent standard error of the mean of three different experiences. The arrows indicate the molecular mass of each isoform. E, CRMP2 processing was analyzed by peptide mass finger printing using MALDI-TOF mass spectrometry analysis of 66, 64, 62, and 58 kDa CRMP2 bands from mouse brain cortex at stages P8 (66, 64, 62 kDa) or P3 (58 kDa). The positions of tryptic peptide sequences matching the CRMP2 internal sequence are indicated in the 66 kDa isoform. When peptide positions are shared, at least in three isoforms, they are only illustrated by a green colored rectangle. When they differ from the tryptic peptide sequences of the 66 kDa isoform, the peptide positions are shown in each specific isoform. The amino acid sequence recovery obtained by peptide mass fingerprinting was 20%, 31%, 18%, and 22% for 66, 64, 62, and 58 kDa CRMP2 isoforms, respectively. F, position of tryptic peptides on the C-terminal part of the CRMP2 amino acid sequence from residues 361 to 572. Underlined sequences indicate matched peptides occurring in at least three isoforms (except for the 533-552 sequence found in both 64 and 66 kDa isoforms). Bold sequences indicate those in common within the short 58 kDa isoform and other isoforms. Note that the most C-terminal tryptic peptide sequences 533-552 and 558-565 were absent from the 58 kDa isoform while present in other isoforms.

Fig. 2. Localization analysis of over-expressed short and full-length CRMP2 isoforms. A, schematic representation of FLAG-tagged full-length and C-terminally truncated CRMP2 ΔC503 constructs used to transfect PC12 cells. Double bars above the lane indicate the position of the tryptic peptide sequence determined in Fig. 1E. B, representative figure shows the expression of full-length CRMP2 or CRMP2 ΔC503, in PC12 cells, by Western blot using anti-FLAG antibody. Note the absence of CRMP2 detection after transfection with the empty vector. C-E, Forty-eight hours after transfection, cells were fixed, treated for immunostaining and viewed using confocal fluorescence microscopy. Representative images from three different experiments are shown. C, transfected cells were double stained with anti-FLAG antibody (green) and phalloidin (red). FLAG expression is co-localized with phalloidin-stained actin for full-length CRMP2 (n= 49). FLAG-CRMP2 ΔC503 shows different staining from actin (n= 103). The later construct is also expressed in the nucleus. No staining with anti-FLAG antibody is observed with the empty vector (as negative control). D, transfected cells were double stained with anti-FLAG (green) and anti-tubulin (red) antibodies. For both full-length and

ΔC503 CRMP2 the anti-FLAG staining overlaps with the anti-α tubulin staining, n=50 per experimental condition. Note that the FLAG-CRMP2 ΔC503 expression is also detected as green staining in the nucleus (merge). E, transfected cells were double stained using anti-FLAG primary antibody followed by an Alexa Fluo 546 anti-rabbit secondary antibody (red), and DAPI (blue). FLAG-tagged full-length CRMP2 is only expressed in the cytoplasm (n= 46), the nucleus is stained blue with DAPI, while FLAG-CRMP2 ΔC503 is expressed in both cytoplasm and nucleus (n= 59), since both show red staining. Scale bars, 15 μm. Typical patterns of staining are shown in high magnification images viewed by confocal fluorescence microscopy.

Fig. 3. Identification of a functional monopartite NLS in CRMP2. A, detailed amino acid sequences of the putative NLS of CRMP2 predicted by database analyses, basic residues are shown by large boxes. B, comparison of the NLS of CRMP2 with amino acid residues of representative NLSs in known nuclear proteins. Bold letters indicate the basic amino acid residues required for nuclear import. C, PC12 cells were transiently transfected with three different FLAG-tagged short CRMP2 ΔC503 constructs bearing mutations within the NLS sequence substituting basic residues with Alanine. The position of each mutation is illustrated in the schematic representation of ΔC503 with respect to the tryptic peptide sequence determined in Fig. 1E. Forty-eight hours after transfection, cells were fixed and double stained with polyclonal anti-FLAG and an Alexa Fluo 546 anti-rabbit antibodies (red), and with DAPI (blue). Scale bars, 25μm. Representative images from three different experiments are shown. Typical patterns of staining are shown in high magnification images. The cells were observed using confocal fluorescence microscopy. The cells expressing mutants K480A+R481A and K483A+R485A+R487A show red staining in both cytoplasm and nucleus. The cells expressing the R471A+K472A construct show an alteration in the nuclear localization of short CRMP2, since the nucleus remains stained blue with DAPI (n=50 for each mutant).

Fig. 4. Surface exposure of the nuclear localization signal motif in CRMP2 structure. A ribbon diagram shows the structure of short CRMP2 from residues 15 to 489. The helices are distinguished by their red color and the strands are in blue. The NLS encompassing residues 471-486 are in green, the functional residues 471-482 are located in a flexible part N-terminal to the α helix. Insert shows the surface representation of short CRMP2, where residues 471-486, colored green, are clearly exposed at the surface.

Fig. 5. Localization of the short CRMP2 isoform in the nuclear fraction of brain tissue. Cerebellar extract from early post-natal stage (P1) brain was subjected to subcellular fractionation in order to separate the different cellular compartments, as indicated in the Experimental Procedures. The representative figure, from three different experiments, shows the presence of 58 kDa isoform by Western blot analysis with anti-pep4 antibody (top panel). The 58 kDa isoform is mainly detected in the nuclear fraction with a faint detection in the cytosol. The arrows on the left indicate the apparent molecular mass of each separate isoform. The 62, 64, and 66 kDa CRMP2 isoforms were detected in cytosol and membrane fractions. Bottom panels show the subcellular identification of each fraction by Western blot analysis, using anti-vimentine, anti-Histone H1, anti-pan cadherin, and anti-HSP70 to identify cytoskeletal, nuclear, membrane, and cytosolic fractions, respectively. Note that anti-HSP70 show a faint detection for membrane fraction.

Fig. 6. Effect of CRMP2 expression on neurite outgrowth. N1E-115 cells were transfected with FLAG-tagged full-length CRMP2, short ΔC503 CRMP2, or NLS-mutated (R471A+K472A) ΔC503 or

full-length constructs. Twenty-four hours post-transfection, cells were cultured in the 5% serum-containing medium for 24 h, fixed and then immunostained with anti-FLAG antibody. A, cells expressing full-length CRMP2 promoted neurite extension, cells expressing the short ΔC503 CRMP2 inhibited neurite extension, and cells expressing ΔC503 CRMP2 bearing mutation in NLS motif restored neurite extension (left panels). Cells expressing full-length CRMP2 with mutated NLS motif promoted neurite extension with no additional induction of neurite elongation (left and lower panels). The images of neuroblastoma cells were captured with Axioplan II microscope showing a staining of the whole cells. Typical patterns of immunostaining are shown in high magnification images on the right panels. Arrows indicate the neurite extension above 20 μm induced by CRMP2. Scale bars, 25 μm. B, cells expressing the empty FLAG-tagged vector (as negative control), viewed by phase contrast microscopy. Scale bars, 25 μm. C, neurite outgrowth in N1E-115 cells, the percentage of cells bearing neurite length >20 μm in transfected cells (n=60 per experimental condition, for one experiment). The values shown are the mean of three independent experiments. Error bars represent standard error of the mean. **, Significantly different from the cells expressing full-length CRMP2 as analyzed by Student's *t* test ($p < 0.001$).

Fig. 7. Effect of CRMP2 expression on primary axon growth. A, Cortical neurons from E15 embryos were plated and maintained in culture without transfection (a) or transfected with FLAG-tagged full-length CRMP2, ΔC503 CRMP2, or ΔC503 CRMP2 mutant R471A+K472A constructs (b-d). They were fixed 2 days after transfection and then immunostained with either anti-CRMP2 (anti-pep4) antibody to visualize the length of axon in non-transfected control cells (a) or anti-FLAG antibody to visualize the entire length of axons in transfected neurons (b-d). Full-length CRMP2 promoted the elongation and branching of the axons, whereas ΔC503 CRMP2 suppressed elongation. Cells expressing ΔC503 CRMP2 (R471A+K472A) bearing NLS mutation restored axon elongation. The neurons were observed with Axioplan II microscope. Arrows indicate primary axons. Scale bar represents 25 μm. B, effect of CRMP2 on axon length. Axon length was measured in non-transfected neurons, and in neurons transfected with each construct in two different experiments (n= 60 per experimental conditions). Data represent the length of axons compared to the control (presenting 92 μm axon length). Error bars represent standard error of the mean. Asteriks indicate the difference from the control neurons expressing endogenous CRMP2 as analyzed by Student's *t* test (* <0.05, ** <0.01).

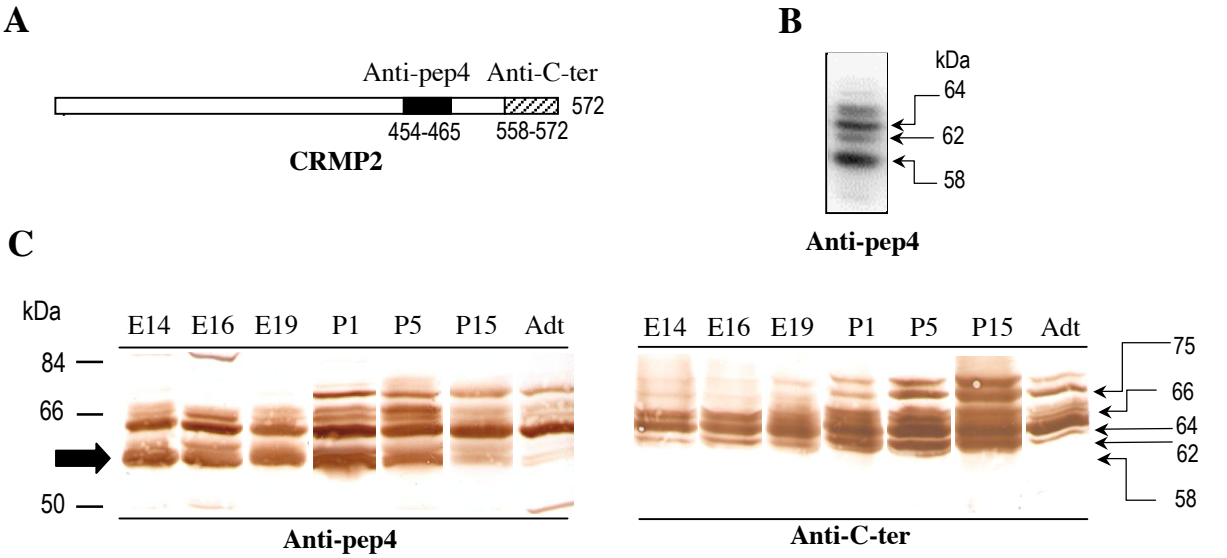

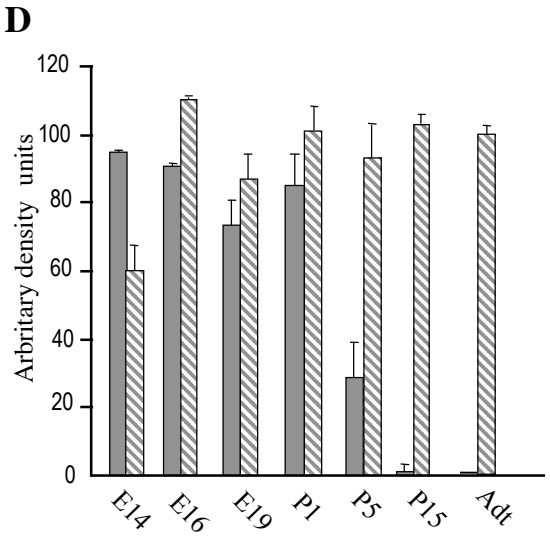

F

361 RMSVIWDKAVVTGKMDENQFVAVTSTNAAK

391**VFNLYPR**397KGRISVGSDADLVIWDPDSVKTI

SAK424**THNSALEYNIFEGMECR**440GSPLVVISQGK

452**IVLEDGTLHVTEGSGR**467YIPR472**KPFPDFVYK**

R481IKARSRLAELRGVPRGLYDGPVCEVSVTPKTV

TPASSAKTSPAKQQAPPVR533NLHQSGFSLSGAQI

DDNIPR552RTTQR558IVAPPGGR565ANITSLG 572

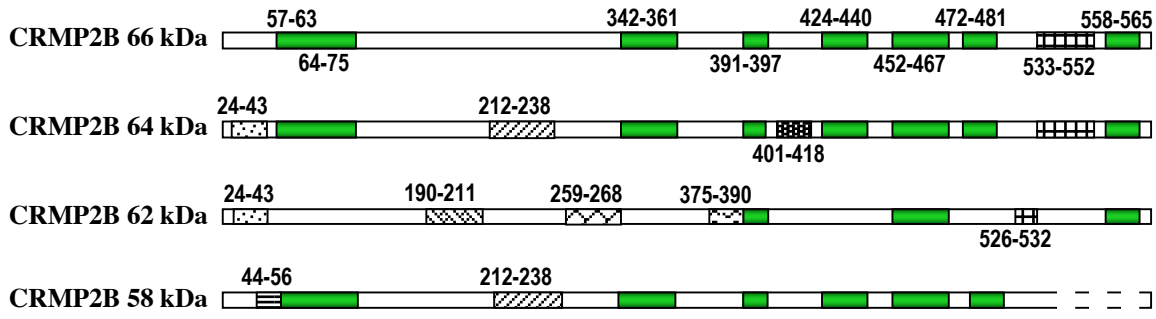

Figure 1

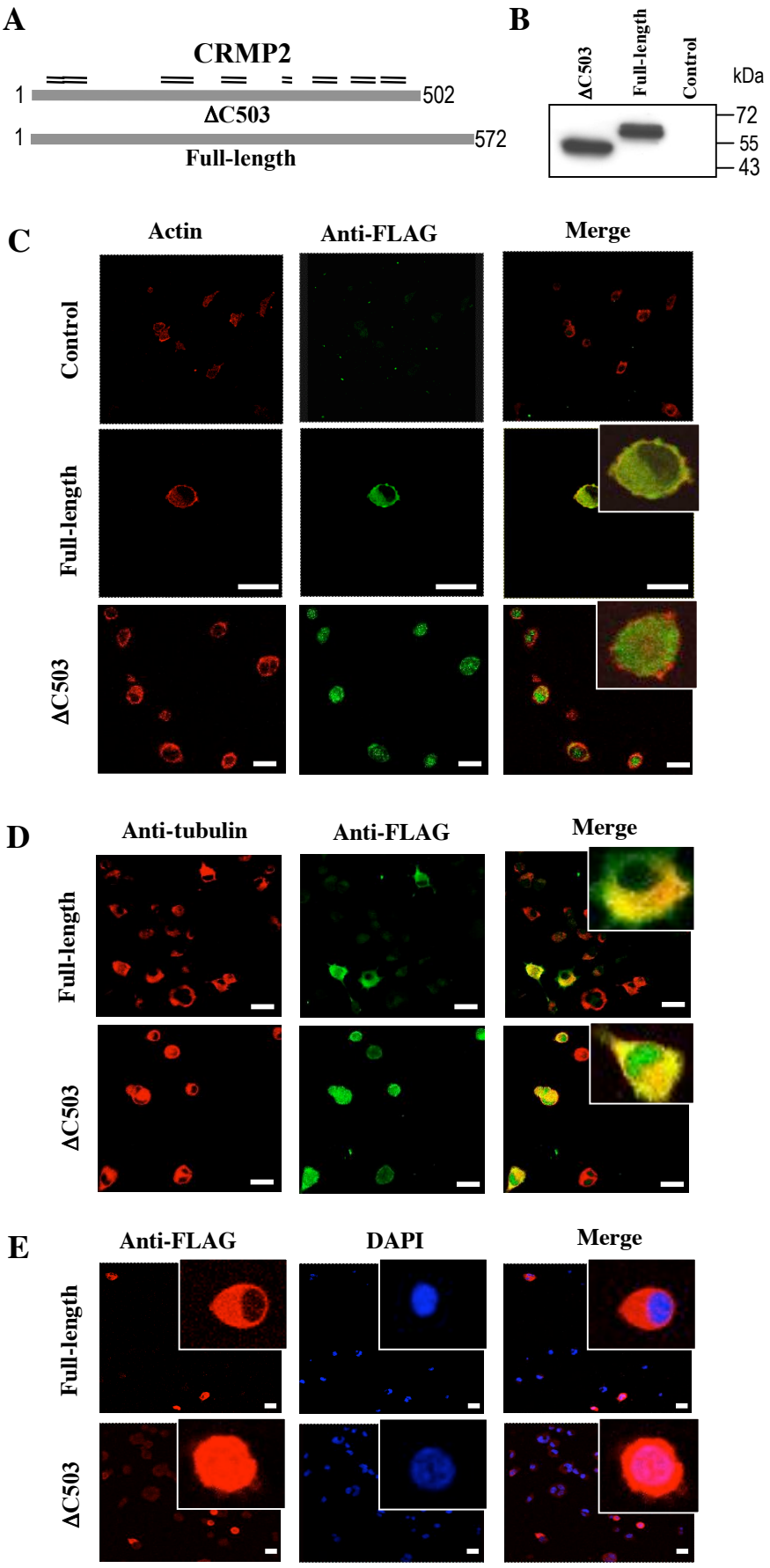

Figure 2

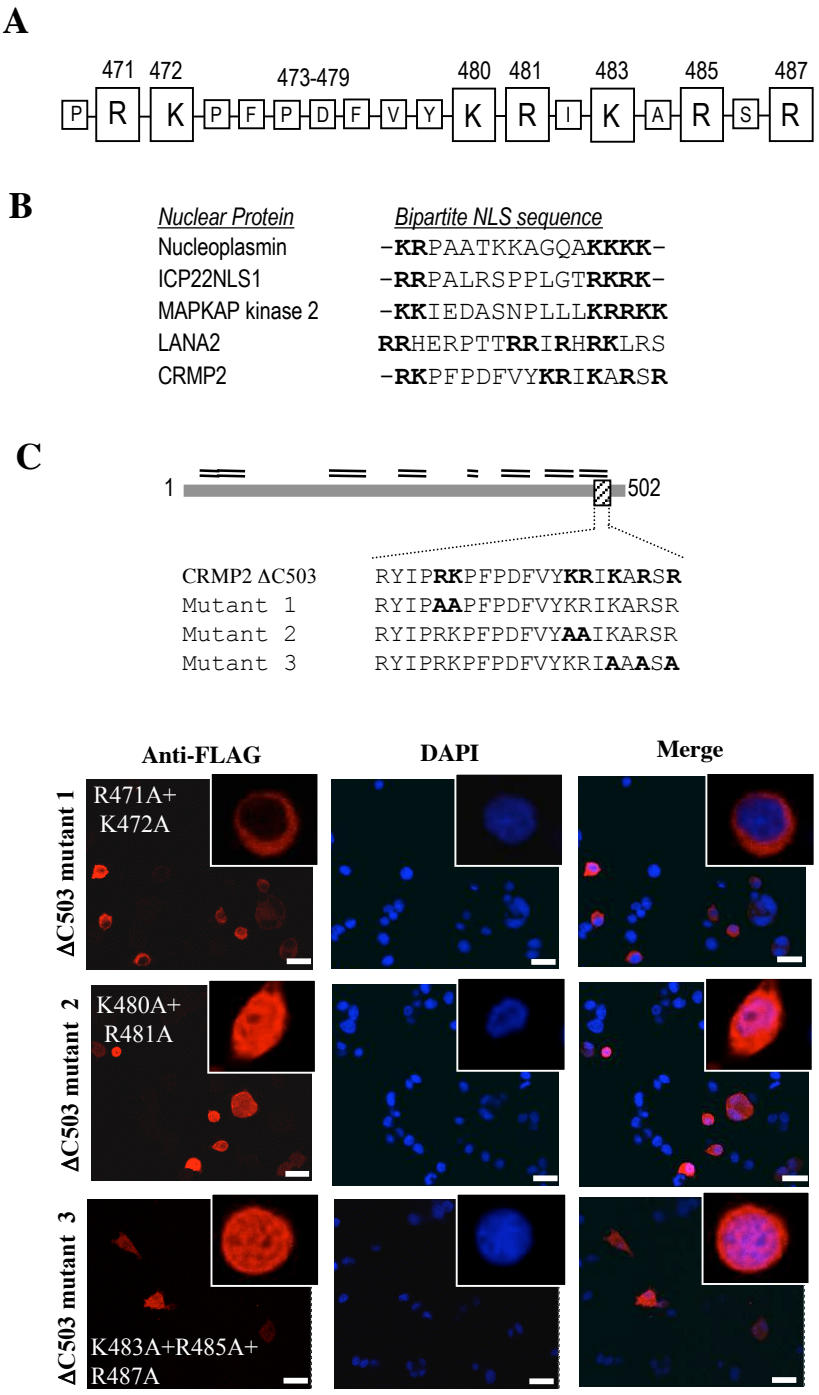

Figure 3

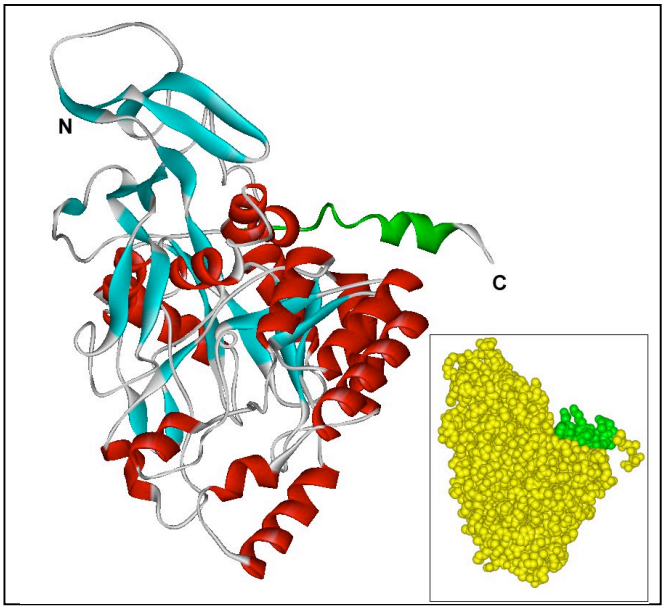

Figure 4

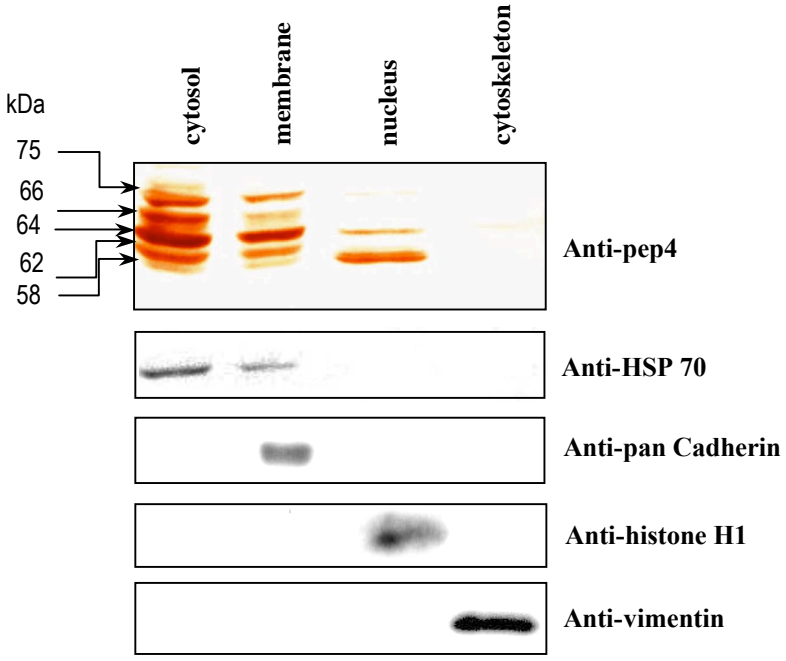

Figure 5

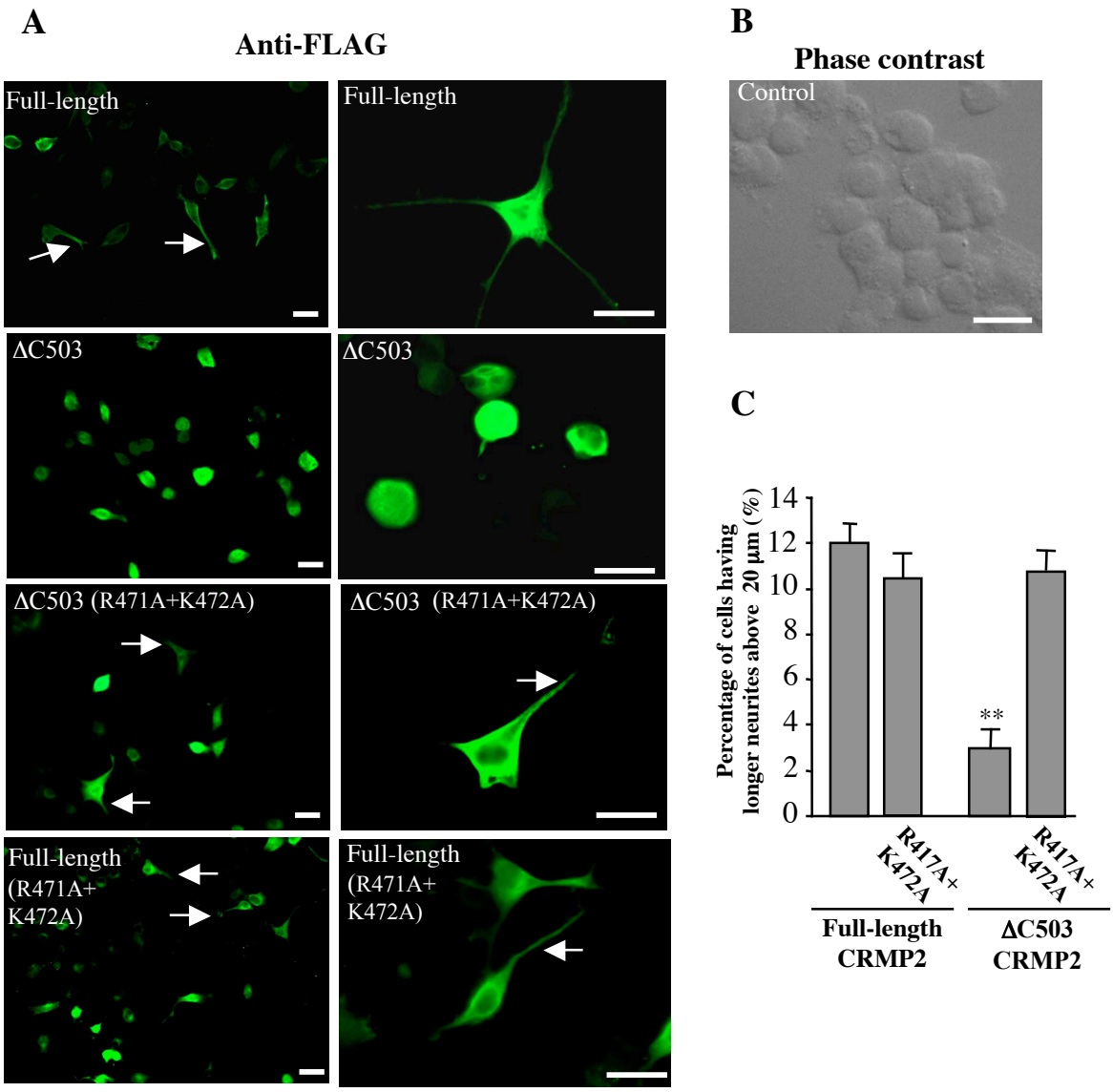

Figure 6

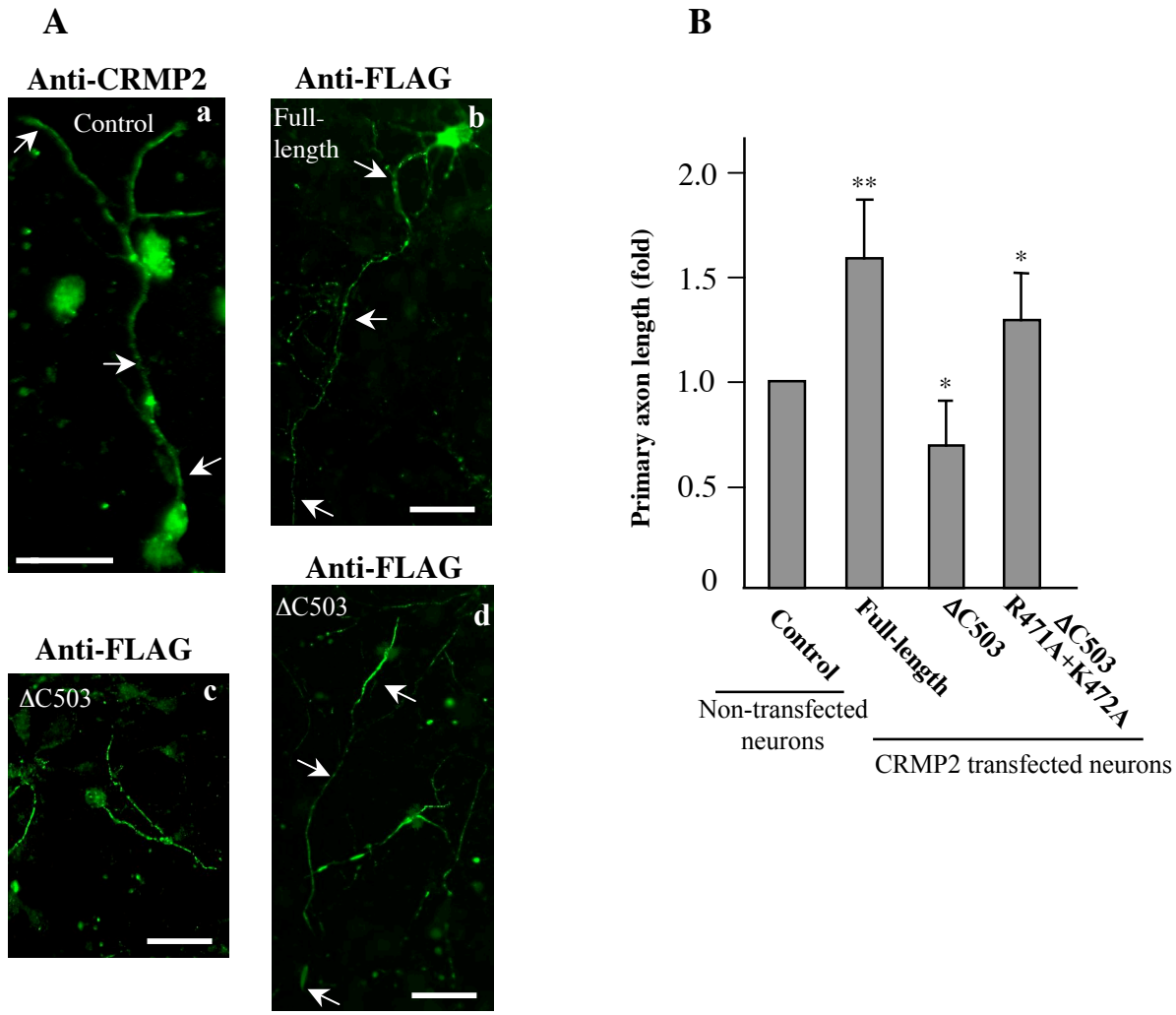

Figure 7